CHEMICAL ENGINEERING TRANSACTIONS
VOL. 117, 2025
A publication of AIDIC
The Italian Association of Chemical Engineering
Online at www.cetjournal.it
Guest Editors: Fabrizio Bezzo, Flavio Manenti, Gabriele Pannocchia, Almerinda di Benedetto

ISBN 979-12-81206-17-5; **ISSN** 2283-9216
DOI: 10.3303/CET25117134

Role of Polypropylene Membranes in Enhancing Lithium Fluoride Crystallization: a Molecular Dynamics Study

Giuseppe Prenesti[a,*], Alfredo Cassano[b], Agostino Lauria[c], Alessio Caravella[a], Francesca Macedonio[b], Elena Tocci [b,*]

[a]Department of Computer Engineering, Modelling, Electronics and System Engineering (DIMES), University of Calabria, Via P. Bucci 42C, 87036 Rende (CS), Italy;
[b]Institute on Membrane Technology–National Research Council of Italy (CNR-ITM), Via P. Bucci 17C, 87036 Rende (CS), Italy
[c]Department of Engineering for Innovation, University of Salento (UNISALENTO), Corpo Z, Campus Ecotekne, SP.6 per Monteroni, 73047 Lecce, Italy
giuseppe.prenesti@unical.it; e.tocci@itm.cnr.it

The increasing demand for lithium in lithium-based batteries (LIBs) underscores the urgent need for sustainable recovery technologies, particularly for recycling exhausted batteries. Membrane-assisted crystallization (MCr) has emerged as a promising method for lithium recovery, enabling the production of high-quality crystals with minimal environmental impact. Although MCr has been widely explored across various applications, its specific role in the crystallization of lithium salts—especially lithium fluoride (LiF)—remains under-researched. This study examines the interactions between LiF solutions and polypropylene (PP) membranes during the crystallization process through molecular dynamics (MD) simulations. By comparing systems with membrane, from now on referring simply as *Membrane*, and without the membrane, from now on referring with the word *Bulk*, we highlight the membrane's pivotal role in influencing water and ion diffusion, promoting ion aggregation, and enhancing crystal formation. The results demonstrate that PP membranes slow water diffusion while facilitating ion mobility, leading to the development of more ordered and crystalline structures. Additionally, interactions with the ionic solution induce subtle morphological changes in the membrane, which influence the spatial arrangement of forming crystals. Experimental validation supports these findings, showing that PP membranes significantly improve crystal quality and structure. This work underscores the essential role of PP membranes in advancing sustainable and efficient lithium recovery technologies.

1. Introduction

The global push to reduce greenhouse gas emissions has led to the adoption of renewable energy sources, but their variability necessitates effective energy storage solutions (Girgibo et al. 2024). Lithium-based batteries (LIBs) are essential for energy storage but contribute to waste and pollution, creating a growing interest in recycling lithium from spent batteries. Techniques such as extraction and reactive crystallization are essential in this process (Ramírez Velázquez et al. 2024). Recovering lithium in crystal form is particularly desirable for reuse, and membrane-assisted crystallization has emerged as a green alternative (Curcio, Criscuoli, and Drioli 2001; Drioli, Di Profio, and Curcio 2012). LiF presents unique challenges due to its low solubility in water, and strong Coulombic interactions between Li^+ and F^-. These characteristics result in significant dehydration barriers, making spontaneous nucleation at room temperature unlikely. Studies have shown that LiF crystallization requires conditions of high supersaturation and typically forms a face-centered cubic (FCC) structure. Hydrophobic polymeric membranes, such as those containing PP, are pivotal in membrane-assisted crystallization, acting as selective barriers that allow water vapor transport while retaining ions. These properties facilitate high-quality crystal recovery while minimizing environmental impact (Frappa, Macedonio, and Drioli 2023; Shen, Dang, and Han 2023). Our recent MD simulation studies revealed that PP membranes exhibit unique interactions with supersaturated LiF solutions, affecting both crystal properties and membrane morphology. These interactions result from the membrane's hydrophobic nature, surface morphology, and

Paper Received: 27 December 2024; Revised: 5 April 2025; Accepted: 23 May 2025
Please cite this article as: Prenesti G., Cassano A., Lauria A., Caravella A., Macedonio F., Tocci E., 2025, Role of Polypropylene Membranes in Enhancing Lithium Fluoride Crystallization: a Molecular Dynamics Study, Chemical Engineering Transactions, 117, 799-804 DOI:10.3303/CET25117134

selective transport properties. This work aims to deepen the understanding of LiF crystallization processes by analyzing the interactions of lithium, fluorine, and water with and without PP membranes. Experimental validation supports the simulation findings, providing insights into the role of PP in controlling crystallization dynamics.

2. Materials and methods

2.1 Computational membrane box

A dense PP model was developed using Materials Studio 8.0. The membrane box dimensions were 50×50×30 Å, achieving a density of 0.85–0.95 g/cm³. The isotactic PP polymer, consisting of 300 monomers with randomized torsion branching, was confined in an amorphous cell containing argon, which acted as a spacer. The box was replicated in a supercell twice in the x and y directions. Two graphene layers (GWs) were positioned on the two largest faces of the box to ensure flat surfaces along the x and y axes. Simulations were conducted using the COMPASS II force field with periodic boundary conditions (Sun et al. 2016). The system was initially optimized for energy and geometry. After optimization, the GWs and argon were removed, and the system was equilibrated under NVT (constant number of molecules, volume, and temperature) and NPT (constant number of molecules, pressure, and temperature) conditions until a stable density was achieved.

2.2 Computational ionic solution

A supersaturated LiF solution was modeled in GROMACS. The system included 8,763 water molecules and a salt concentration of 8.9 M. The solution box dimensions were 50×50×108.3 Å, later reduced to 43.3×43.3×93.9 Å after equilibration. The OPLS-AA force field (Doherty et al. 2017) and SPC/E (Yuet and Blankschtein 2010) water model were used, with systems equilibrated under NPT conditions for 1 ns at 300 K and 1 bar.

2.3 Computational membrane-solution system

The PP membrane and ionic solution were initially placed with a small gap to avoid overlap. After performing energy minimization and NPT equilibration, the system converged, eliminating the initial gap between the solution and membrane. MD simulations were then extended for 800 ns under NPT conditions, using the V-rescale thermostat for temperature control and the Particle Mesh Ewald (PME) method to handle long-range electrostatic interactions. The analysis focused on diffusion coefficients and coordination numbers to monitor crystallization. The number of atoms and the dimensions of each simulation box are summarized in Table 1. Concentration were chosen according to literature data (Lanaro and Patey 2018).

Table 1: Simulation box parameters for different conditions.

Conditions	n. Li^+	n. F^-	n. water	n. PP	n. total atoms	Box dimensions (nm)
Bulk (1)	1451	1451	17583	-	20485	4.43×4.43×9.59
Bulk (2)	1451	1451	17583	-	20485	4.44×4.44×9.61
Membrane (1)	1451	1451	17583	10808	31293	4.76×4.76×13.5
Membrane (2)	1451	1451	17583	10808	31293	4.74×4.74×13.4

The computational parameters were consistent with the earlier steps. The equilibrated system underwent 800 ns of simulation under NPT conditions, where the V-rescale thermostat and Berendsen barostat were employed to maintain a temperature of 300 K and pressure of 1 bar. Coulomb and van der Waals interactions were calculated using a 1.0 nm cut-off, with long-range interactions handled via PME (Petersen 1995). Covalent bonds in water were constrained using the LINCS algorithm (Hess et al. 1997).

2.4 Crystals data analysis

A detailed data analysis approach was developed to track crystal formation within the simulations by processing ion trajectories. The method includes three key steps (Lanaro and Patey 2016): 1) Ion Filtering: The Steinhardt order parameter was used to classify ions based on their local environment, categorizing them as solid-like or liquid-like. 2) Crystal Identification: The DBSCAN machine learning algorithm was applied to group solid-like ions into clusters, identifying potential crystals. 3) Crystal Stability Evaluation: The Jaccard similarity index was calculated to assess the stability and persistence of crystals over time. Additionally, self-diffusion coefficients (D_i) for all species were determined using the long-time limit of the Mean Square Displacement, applying the Einstein relation as shown in Equation 1 (Perrotta et al. 2020):

$$D_i = \lim_{t\to\infty} \frac{\left\langle \left| r(t) - r(0) \right|^2 \right\rangle}{6t} \tag{1}$$

where *r(t)* is the position vector (nm) of the center of mass of the molecule (or ion) at time *t (ns)*.
The coordination number (CN) was calculated using Equation 2 (Perrotta et al. 2020):

$$CN = 4\pi\rho\int_{0}^{r_c} r^2 g(r) dr \quad (2)$$

where ρ is the molecular density (number of molecules nm^{-3}), *g(r)* (-) is the radial distribution function (rdf), *r* is the position (nm) and r_c is the position (nm) of the first minimum after the first pick.

2.5 Experimental methodology

Solutions were prepared by dissolving lithium fluoride (LiF) in ultra-pure water to a concentration of 1.012×10^{-3} g mL^{-1}. Hydrophobic flat-sheet polypropylene membranes are sourced from 3M. All tests were performed in a climate-controlled room at 300 K and 60% humidity. The experiments included placing 15 µL drops in a glass petri plate without a membrane or on a PP membrane. Crystals' formation is monitored via microscope (Nikon eclipse LV100ND) images.

3. Results and discussions

The presence of the membrane significantly impacts the self-diffusion coefficients of all species, causing a reduction during the initial 50 ns compared to simulations without the membrane. This behaviour aligns with our prior findings indicating that the membrane acts as a barrier, controlling ion aggregation and nucleation events. Self-diffusion coefficients in our study are lower than those calculated in an under-saturated LiF solution (D_{Li+} (300K) = 1.188 ± 0.039 10^{-5} cm^2 s^{-1}) (Errougui and Benbiyi 2021), further confirming reduced mobility and its role in promoting aggregation and nucleation. A similar mobility reduction is evident during induced LiF bulk crystallization, where D_{Li+} (300K) =1.90±0.07 10^{-7} cm^2 s^{-1} (Lanaro and Patey 2018). A key focus lies in the changes observed after crystal formation, particularly at the end of the simulations. Figures *1*a and *1*b illustrate the diffusion coefficients of all species during the final 50 ns of the simulations (750–800 ns). In both systems, the diffusion coefficients of ions are significantly reduced compared to the initial phase (0–50 ns), indicating increased ion aggregation into crystals. This aggregation results in stronger ionic interactions, which limit ion mobility. In contrast, water diffusion coefficients increase in both systems, reflecting the need for water to exit the ions' solvation shells during crystal formation. The reduction in ion diffusion is more pronounced in the bulk system compared to the membrane system (Table 2). The membrane enables subtle ion rearrangements, promoting more ordered crystals through controlled interactions with the polymeric matrix, enhancing crystallization efficiency.

Table 2: *Percentage variation in Water and Ion Diffusion Coefficients between 0 ns and 800 ns.*

Species	ΔD % Bulk	ΔD % Membrane
Water (bulk)	117	118
Lithium (bulk)	-67	-55
Fluorine (bulk)	-68	-56

The relationship between diffusion and aggregation was further analyzed by calculating the coordination number (CN) to understand the organization of lithium, fluorine, and water molecules. CN was determined for Li-F and Li-OH_2 interactions (Figure 1c, d). Over time, CN_{Li-F} increased while CN_{Li-OH2} decreased. This shift reflects lithium and fluorine ions coming closer to form ordered crystal structures. These results are consistent with the FCC crystal structure, where each lithium atom is surrounded by six fluorine atoms. Although our simulations did not reach the theoretical CN value of six, the observed crystallization dynamics align with experimental data, which suggest CN values between four and six. First-principle MD simulations for low-concentration systems also report CN~4, consistent with our findings (Ikeda, Boero, and Terakura 2007). Bulk crystallization achieved a CN of approximately 3, whereas membrane-assisted crystallization resulted in a CN of 4.6. These results indicate that interactions between the membrane and the solution encourage lithium desolvation, promoting ion aggregation and enhancing crystallinity. Figures *1*e and *1*f illustrate the probability density functions (PDF) of crystallinity for the bulk and membrane-assisted systems at the conclusion of the simulations. Crystallinity, assessed using the mean Steinhardt parameter, quantifies lattice order, with higher values reflecting a more perfect structure. A crystallinity value of 0.41, calculated for a perfect crystal of 1,700 atoms (blue dotted line in Figures 1e and 1f), serves as a benchmark for evaluating crystal quality in the simulations. The presence of the membrane shifts the crystallinity distribution towards higher values, highlighting its significant role in enhancing crystal order. Crystals in the bulk system show lower crystallinity, beginning with disordered structures caused by the chaotic growth environment. In contrast, membrane-assisted crystals exhibit higher initial order, with the

gap in crystallinity between the two systems widening over time. The PDF analysis confirms a progressive shift toward higher crystallinity in the membrane system, underscoring its ability to regulate crystal formation. The membrane provides precise control of the supersaturation environment, acting as a structured interface that guides ion aggregation into well-ordered lattices. This reduces randomness in ion motion, producing stable, uniform crystals. Conversely, the bulk system's dynamic, unregulated environment results in smaller, less ordered crystals.

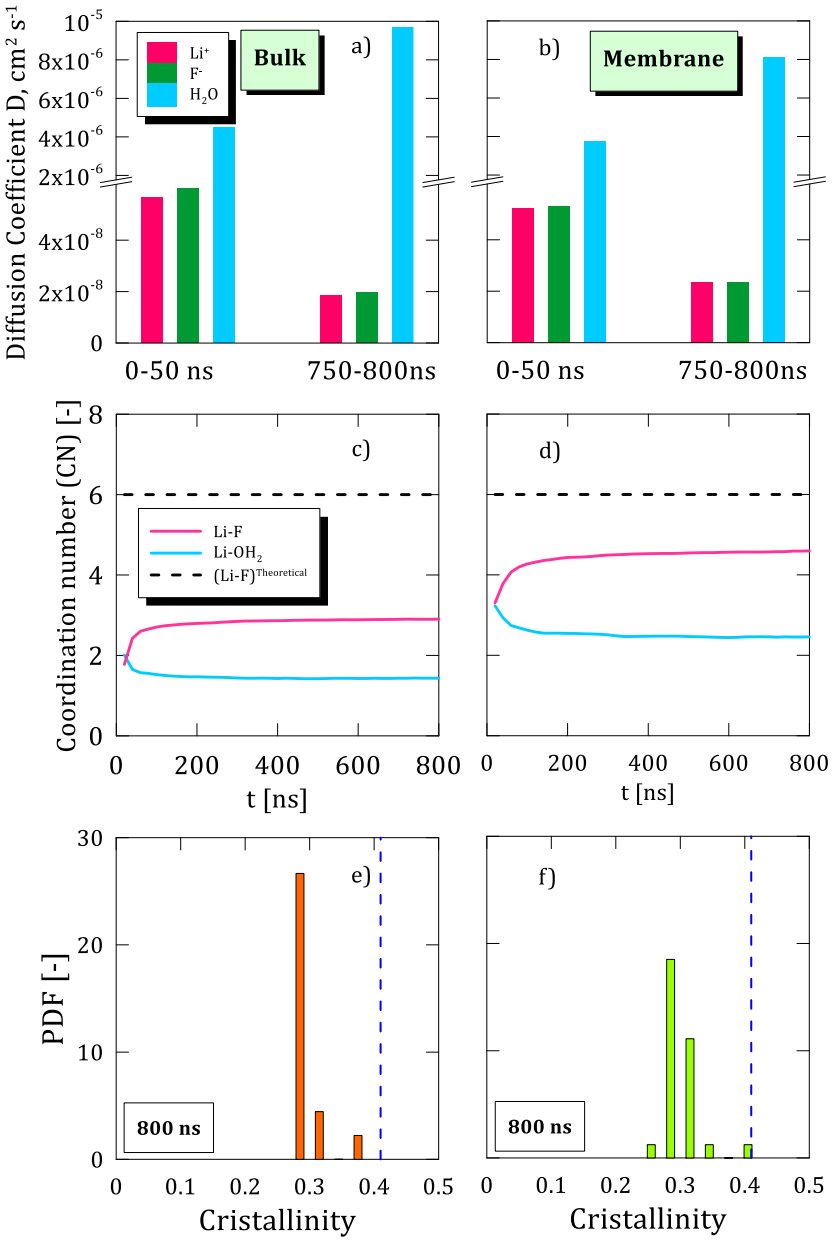

Figure 1:a) Diffusion coefficients of all species in the bulk system. b) Diffusion coefficients of all species in the membrane system. c) Lithium coordination with fluorine (pink curve) and water oxygen (blue curve) in the bulk system. d) Lithium coordination with fluorine (pink curve) and water oxygen (blue curve) in the membrane system. e) Probability density function (PDF) of crystallinity for the bulk system. f) PDF of crystallinity for the membrane system. The blue dotted line represents a crystallinity value of 0.41, which corresponds to a perfect crystal containing 1,700 atoms.

Experimental validation revealed that crystal formation occurs faster in the absence of the membrane (*Bulk*: 18±5 min, *Membrane*: 78±5 min). However, this rapid crystallization leads to less ordered and more aggregated crystals, highlighting the importance of the simulation results. The slower water diffusion observed in the presence of the membrane enables reduced ion motion, resulting in the formation of more ordered crystals.

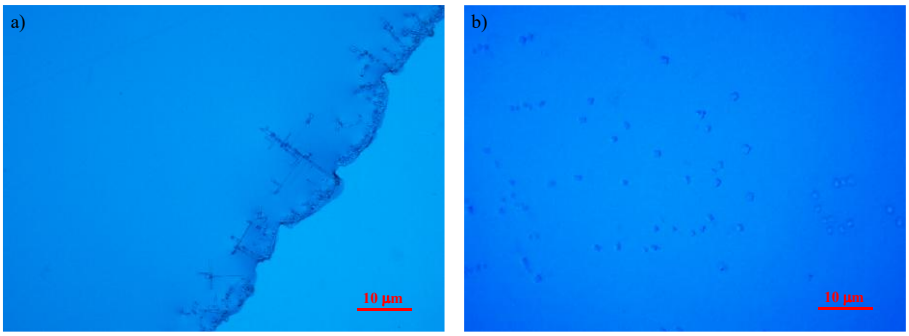

Figure 2. a) Crystals in the bulk (magnification x20). b) Crystals in the membrane system (magnification x20).

Figure 3 compares crystal morphology in the bulk and membrane systems. The membrane system produces more uniform and structured crystals, further confirming its role in enhancing crystallinity. The membrane system produces more uniform and structured crystals, further confirming its role in enhancing crystallinity.

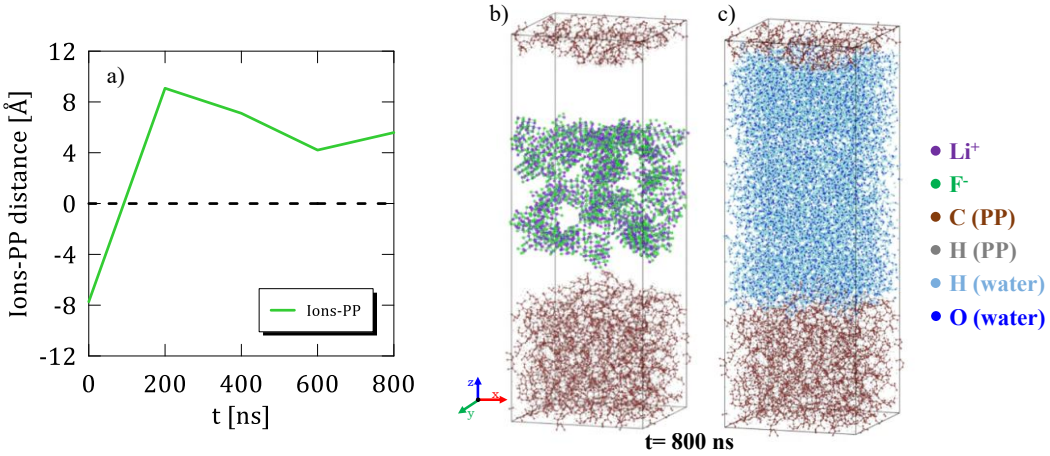

Figure 4. *a) Time profile of ion-PP distances along the z-direction. b) Positions of ions and PP at 800 ns. c) Positions of water and PP at 800 ns.*

The membrane's morphology was also analyzed (Figure 5). Our previous studies indicate that polymeric chains undergo slight shrinkage, reducing the membrane's total volume. This shrinkage allows water to accumulate near the membrane surface without being adsorbed. Figure 4a shows the time profile of the distance along the z-direction between the nearest ion and the PP membrane. Initially, negative values reflect valleys formed by deformed polymeric chains, which host ions and water. As crystals begin to form, they grow away from the membrane surface, increasing the distance before stabilizing at nonzero values. This behavior aligns with the hypothesis that water acts as a buffer, mitigating the membrane's superficial charge and facilitating controlled crystal growth. Figures 4b and 4c further illustrate the system's behavior at the end of the simulation (800 ns). Figures depicts the relative positions of ions and the membrane, while Figure 4c highlights the distribution of water near the membrane surface. Crystals form within the solution, maintaining a controlled proximity to the membrane, supported by a thin water film. This film prevents excessive interaction with the surface, ensuring a more stable and predictable growth environment.

4. Conclusions

This study utilized MD simulations to investigate the early stages of the crystallization process in systems with and without a polypropylene membrane. A comprehensive data analysis strategy was implemented to identify ions with solid-like characteristics, group them into crystals based on defined parameters, and track their stability over time. The primary objective was to elucidate the influence of the polymeric membrane on the crystallization process. The results demonstrate that interactions between the ionic solution and the PP membrane significantly enhance crystal crystallinity. This enhancement is attributed to the membrane's modulation of diffusion coefficients for both ions and water. Initially, the PP membrane acts as a barrier, slowing water motion and delaying ion diffusion. This delay promotes controlled ion desolvation and aggregation. Over time, the

membrane facilitates increased ion diffusion, enabling the reorganization of aggregated ions into more ordered crystal structures. These dynamics are reflected in the coordination number between lithium and fluorine, which is notably higher in the presence of the membrane compared to the bulk system. Experimental validation confirmed these findings. Tests conducted in static conditions demonstrated that the presence of the PP membrane prevents the formation of disordered and overly aggregated crystals, thereby corroborating the simulation results. Furthermore, it was observed that the ionic solution interacts with the membrane, inducing a slight shrinkage of the polymeric chains. This morphological change allows water to approach the polymer surface without being adsorbed, effectively mitigating the surface charge of the PP membrane and facilitating controlled crystal formation. In conclusion, the PP membrane plays a dual role in the crystallization process: it modulates diffusion rates to promote controlled nucleation and enhances the final crystallinity and order of the resulting crystals. These findings underline the critical role of PP membranes in membrane-assisted crystallization and their potential for improving sustainable lithium recovery technologies.

Acknowledgments

This work was funded by the Next Generation EU - Italian NRRP, Mission 4, Component 2, Investment 1.5, call for the creation and strengthening of ‘Innovation Ecosystems', building ‘Territorial R&D Leaders' (Directorial Decree n. 2021/3277) - project Tech4You - Technologies for climate change adaptation and quality of life improvement, n. ECS0000009.
We acknowledge ISCRA for awarding this project access to the LEONARDO supercomputer, owned by the EuroHPC Joint Undertaking, hosted by CINECA (Italy).

References

Curcio, E., A. Criscuoli, and E. Drioli., 2001, Membrane Crystallizers, Industrial and Engineering Chemistry Research, 40, 2679–84.

Doherty, Brian Xiang Zhong, Symon Gathiaka, Bin Li, Orlando Acevedo, 2017, Revisiting OPLS Force Field Parameters for Ionic Liquid Simulations, Journal of Chemical Theory and Computation, 13, 6131–35.

Drioli, Enrico, Gianluca Di Profio, and Efrem Curcio., 2012, Progress in Membrane Crystallization, Current Opinion in Chemical Engineering, 1, 178–82.

Errougui, Abdelkbir, and Asmaa Benbiyi., 2021, Molecular Dynamics Simulation of Lithium Fluoride in Aqueous Solutions at Different Temperatures 300 K - 360 K, E3S Web of Conferences, 229, 0–5.

Frappa, Mirko, Francesca Macedonio, and Enrico Drioli. 2023, Membrane-Assisted Crystallization.

Girgibo Nebiyu, Hiltunen Erkki, Lu Xiaoshu, Makiranta Anne, Tuomi Ville, 2024, Risks of Climate Change Effects on Renewable Energy Resources and the Effects of Their Utilisation on the Environment, Energy Reports, 11, 1517–34.

Hess, Berk, Henk Bekker, Herman J.C. Berendsen, and Johannes G.E.M. Fraaije., 1997, LINCS: A Linear Constraint Solver for Molecular Simulations, Journal of Computational Chemistry, 18, 1463–72.

Ikeda, Takashi, Mauro Boero, and Kiyoyuki Terakura., 2007, Hydration of Alkali Ions from First Principles Molecular Dynamics Revisited, Journal of Chemical Physics, 126.

Lanaro, G., and G. N. Patey., 2016, Birth of NaCl Crystals: Insights from Molecular Simulations.” Journal of Physical Chemistry B, 120, 9076–87.

Lanaro, G., and G. N. Patey., 2018, The Influence of Ion Hydration on Nucleation and Growth of LiF Crystals in Aqueous Solution, Journal of Chemical Physics, 148.

Perrotta Maria Luisa, Macedonio Francesca, Giorno Lidietta, Jin Wanqin, Drioli Enrico, Gugliuzza Annarosa, Tocci Elena, 2020, Molecular Insights on NaCl Crystal Formation Approaching PVDF Membranes Functionalized with Graphene, Physical Chemistry Chemical Physics, 22, 7817–27.

Petersen, Henrik G., 1995, Accuracy and Efficiency of the Particle Mesh Ewald Method, The Journal of Chemical Physics, 103, 3668–79.

Ramírez Velázquez, L. E., Laëtitia Palos, Marie Le Page Mostefa, and Hervé Muhr., 2024, Recovery of Lithium from Li-Ion Battery Leachate by Gas-Liquid Precipitation, Journal of Crystal Growth, 631.

Shen, Lixia, Mingyan Dang, and Xingwei Han., 2023, Recent Advances in Membrane Crystallization, CrystEngComm, 25, 2503–17.

Sun Huai, Jin Zhao, Yang Chunwei, Akkermans Reinier L. C., Robertson Struan H., Spenley Neil A., Miller Simon, Todd Stephen M., 2016, COMPASS II: Extended Coverage for Polymer and Drug-like Molecule Databases, Journal of Molecular Modeling, 22, 1–10.

Yuet, Pak K., and Daniel Blankschtein., 2010, Molecular Dynamics Simulation Study of Water Surfaces: Comparison of Flexible Water Models, Journal of Physical Chemistry B, 114,13786–95.